

Cascade mechanism in a self-regulatory endocrine system. Modeling pulsatile hormone secretion*

Thongchai Dumrongpokaphan and Yongwimon Lenbury[‡]

Department of Mathematics, Faculty of Science, Mahidol University, Thailand

Abstract: Many endocrine systems have been found to incorporate some form of cascade mechanism into their operation. Such a mechanism involves an amplification system where an initial reaction gives rise to the generation of multiple second reactions, each of which sets off multiple third reactions, and so on. Examples will be presented, with special attention paid to the hypothalamus–pituitary–testicular axis. The production and secretion of luteinizing hormone (LH) is governed by the medial-basal region of the hypothalamus. It is well known that the release of LH is a highly regulated process determined by negative and positive feedback, as well as neural components. The presence of gonadotropin-releasing hormone (GnRH) on specific adenohypophyseal cell membrane receptors results in the release of LH, which is then transported systemically to the Leydig cells of the testes. All the factors governing the release of these hormones, as well as a biochemical description of their actions, have not been completely elucidated, nor is the mechanism behind the pulsatile fashion in which the decapeptide GnRH and LH are released clearly explained. We describe how such a cascade mechanism in a self-regulatory system may be modeled and analyzed by a singular perturbation approach, identifying conditions that give rise to episodic hormone secretion or activity. Insightful and valuable interpretations can be made from such analysis of the cascade system.

INTRODUCTION

In recent years, there has been a great surge of interest in the study of how information is represented and transmitted in biological systems, specifically in the new field of bioinformatics. In nerve cells, information is transmitted through electrical impulses, which are sometimes generated as high-frequency bursts, followed by periods of quiescence. These impulses also cause muscles to contract and endocrine cells to secrete hormones. Quite often, bursting or episodic activities are observed in biological systems, particularly in endocrine cells. Attempts to model and simulate such mechanisms most frequently lead to nonlinear differential equations. This presents us with quite a challenge to develop nonlinear systems theory and analytical techniques to qualitatively and quantitatively unravel the intrinsic mechanisms that generate such behavior in these complex systems.

The study of endocrinology over the past century has been mainly dependent upon the scientific methodologies available to probe the various endocrine systems. Thus, endocrinology has developed from being largely pursued at the physiological level into a biochemical era, which began in approximately 1955–1960 [1] and extends to the present time. Advances in chemical methodology, such as chromatography, mass spectrometry, nuclear magnetic resonance spectroscopy (NMR), and X-ray crystallography, have and continue to permit the detection and chemical characterization of minute quantities (nanograms or picograms) of new hormones and the characterization of the many receptors.

*Plenary lecture presented at the International Conference on Bioinformatics 2002: North–South Networking, Bangkok, Thailand, 6–8 February 2002. Other presentations are presented in this issue, pp. 881–914.

[‡]Corresponding author

With the invention of scanning electron microscopes and confocal microscopy, which allows real-time imaging of living cells, the science of endocrinology is advancing rapidly. Scientists have been busily active in categorizing and defining the scope of influence and molecular mode of action of different hormones, as well as the mechanisms in their secretion.

Many endocrine systems incorporate some form of cascade mechanism into their operation [1]. A system with a cascade mechanism is an amplification process where an initial reaction results in the generation of multiple second reactions, each of which sets off multiple third reactions, and so on.

In this paper, we first discuss two examples of such cascade systems and explain how modeling and analysis of the system may be carried out based on singular perturbation principles. The method utilizes simple geometric arguments based on the assumption of highly diversified dynamics inherent to the cascade system. Application of the technique is done on the hypothalamus–pituitary–testicular axis involved in the biosynthesis and secretion of testosterone in response to blood levels of luteinizing hormone (LH). Episodic release of LH is triggered by the presence of the gonadotropin-releasing hormone (GnRH), secreted from the hypothalamus in a pulsatile fashion [1,2], which we attempt to explain through modeling and analysis. The analysis will then be extended to encompass higher-dimensional systems, which involve a multitude of components or species.

CASCADE HORMONE SYSTEMS

In the following, we describe two examples of systems with cascade mechanism. One classical biochemical cascade mechanism, at the cellular and molecular level, is generated by the action of a hormone, such as the action of glucagon at the cell membrane to produce an increase in cyclic AMP. Figure 1 shows a schematic description of a mechanism leading from the cell surface hormonal signal to the cellular metabolic response: glucagon and glycogenolysis. The cascade may be visualized in terms of alter-

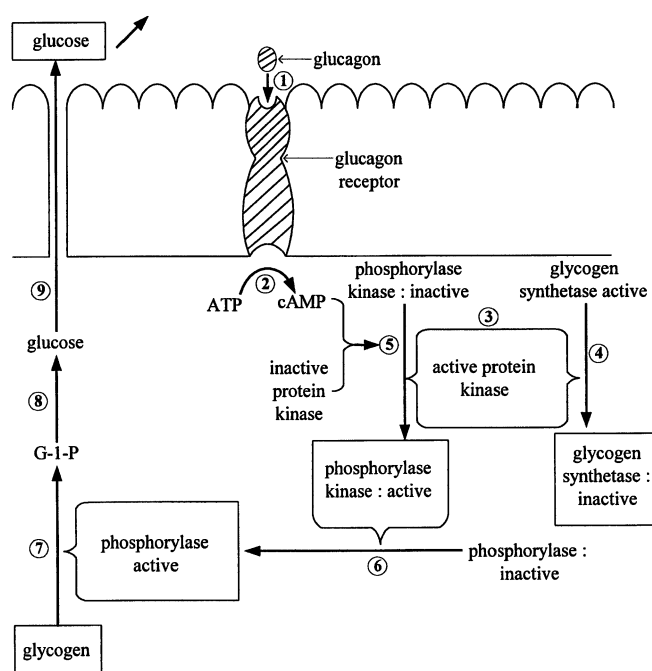


Fig. 1 A schematic description of a mechanism leading from the cell surface hormonal signal to the cellular metabolic response: glucagon and glycogenolysis.

ations of cellular response, stimulation of glycogenolysis to generate glucose for export to the extracellular space, and the general circulating system [1].

As so clearly elucidated by Norman and Litwack [1], the cascade begins with glucagon combining with its cell membrane receptor, marked (1) in Fig. 1. This then stimulates the activity of adenylate cyclase, possibly mediated by a transducing element, on the cytoplasmic side of the membrane, marked (2) in Fig. 1. As a result, the level of cyclic AMP increases, which activates a protein kinase (3), while the protein kinase subunits catalyze the phosphorylation of inactive phosphorylase kinase in reaction (5), as well as the active glycogen synthetase (4), to produce the phosphorylated inactive form, a step marked (6) in Fig. 1. The resulting phosphorylated inactive form consequently stimulates glycogenolysis in step (7) to form glucose 1-phosphate, which is further metabolized to glucose (8). Finally, glucose is transported to the extracellular space and into the general circulation (9). More detailed discussion of each step in the above-described cascade may be found in the work by Norman and Litwack [1]. The system is considered a cascade system due to the fact that each step following hormone binding is mediated by an enzyme that can turn over multiple substrate molecules.

Another system, which also incorporates the cascade mechanism, involves the central nervous system (CNS), the hypothalamus, pituitary, and the distal hormone secretion glands.

As explained by Norman and Litwack in their seminal work on hormones [1], the cascade effect may be produced by a single event or signal in the external or internal environment. A signal can be sent by either electrical or chemical transmission to the limbic system and then to the hypothalamus. This results in the secretion of a releasing hormone into the closed portal system connecting the hypothalamus and anterior pituitary shown in Fig. 2. It has been documented that releasing hormones may be secreted in nanogram amounts and half-lives of about 3–7 min. The releasing hormone consequently

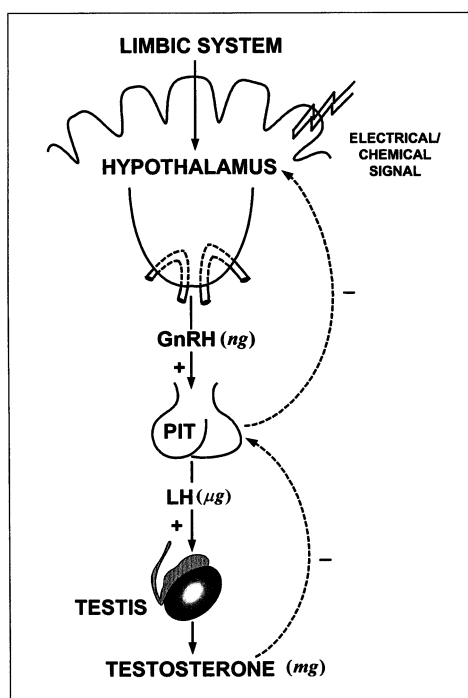


Fig. 2 Diagram showing the cascade hormonal system, the hypothalamus–pituitary–testicular axis, on proceeding down the cascade from the releasing hormone to the terminal hormone, there are increasing masses of the hormones released.

signals the release of the specific anterior pituitary hormones, which may be secreted in microgram amounts with half-lives on the order of 20 min or longer. The anterior pituitary in turn signals the release of the ultimate hormone, which may be secreted in many micrograms or milligram amounts and can be quite stable.

Thus, amplification of a single event at the outset could prove to be a factor of thousands to a millionfold, as hormone stability and the amounts of hormones increase as we proceed down the cascade.

Three-component cascade system

Letting $x(t)$, $y(t)$, and $z(t)$ represent the densities or levels of the three components at anytime t in the cascade system described above, their rates of production will form a model consisting of the following system of differential equations

$$\dot{x} = f(x, y, z) \quad (1)$$

$$\dot{y} = \varepsilon g(x, y, z) \quad (2)$$

$$\dot{z} = \varepsilon\delta h(x, y, z) \quad (3)$$

where ε and δ are small positive parameters. Thus, when the quantities on the right sides of eqs. 1–3 are finite and different from zero, $|\dot{y}|$ is of the order ε and $|\dot{z}|$ is of the order $\varepsilon\delta$. Thus, x is assumed to possess the fastest dynamics, y an intermediate time response, while z possesses the slowest dynamics of the three components.

It is well known that the system (1–3) with small ε and δ can be analyzed with the singular perturbation method [3], which under suitable regularity conditions, allows the approximation of the solution of the system (1–3) with a sequence of simple dynamic transitions occurring at different speeds.

Given an initial condition (x_0, y_0, z_0) , the slow z and intermediate (y) variables are frozen, and the system will develop according to the “fast system”.

$$\dot{x}(\tau_1) = f[x(\tau_1), y_0, z_0] \quad , \quad \tau_1 = \frac{t}{\varepsilon\delta}$$

Thus, $x(\tau_1)$ eventually tends toward a stable equilibrium $\bar{x}(x_0, y_0, z_0)$ of the fast system. Then, as z is still frozen at z_0 , the transitions will develop at intermediate speed according to the “intermediate system”

$$\dot{y}(\tau_2) = g\{\bar{x}[x_0, y(\tau_2), z_0], y(\tau_2), z_0\} \quad , \quad \tau_2 = \frac{t}{\varepsilon}$$

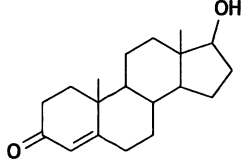
until an equilibrium $\bar{y}(x_0, y_0, z_0)$ of the intermediate system is reached. A third transition then develops at low speed along the curve $f = g = 0$ to end at an equilibrium or form a closed cycle, depending on the stability properties of the three equilibrium manifolds $f = 0$, $g = 0$, and $h = 0$.

The sequence of these transitions thus constructed then approximates the solution of the system, in the sense that the real trajectory is contained in a tube around the traced transitions, and that the radius of the tube goes to zero with ε and δ . More detail of the main aspects of the method can be found in the work by Muratori and Rinaldi [3], while examples of applications to nonlinear systems in biology and medicine are available in the works of Lenbury et al. [4,5].

Application in modeling pulsatile secretion of LH

The hypothalamus–pituitary–testicular axis is diagrammed schematically in Fig. 2. The release of LH is a highly regulated process determined by (a) negative feedback, (b) positive feedback, and (c) neural components.

Table 1 Relevant information on testosterone.

Biochemical aspects	Data
Plasma concentration (ng/100 ml)	300–1100
Testes secretion rate	5000
Metabolic clearance rate (litre/day)	980
Site of production	Leydig cells of testes
Structure	
Principal biological function	Maintenance of functional male reproductive system and secondary male sex characteristics

The decapeptide GnRH is released from the hypothalamus in a pulsatile fashion with short latency and initiates the episodic secretion of LH. The LH is then transported systemically to the Leydig cells of the testes. LH-mediated stimulation of testosterone synthesis and secretion by the Leydig cells is initiated by the binding of LH to hormone-specific receptors on the outer membranes of the Leydig cell. The rate of biosynthesis and secretion of testosterone, whose structure is shown in Table 1, is positively correlated with the blood levels of LH, while the secretion of the gonadotropin can be diminished by increasing blood concentrations of testosterone, which facilitates their binding to steroid receptors in both the hypothalamus and pituitary. This is called “suppressive negative feedback”. The precise details of the feedback mechanism in this self-regulatory system are not yet clear. Nevertheless, close study of the process has led Liu and Deng [6] to propose a model consisting of the following equations.

$$\frac{dR}{dt} = \frac{a_1 + a_2R + a_3R^2}{1 + \alpha_4T + \alpha_5T^2 + a_6R + a_7R^2} - a_8R \quad (4)$$

$$\frac{dL}{dt} = \frac{a_9 + a_{10}R}{1 + a_{11}T + a_{12}R} - \alpha_{13}L \quad (5)$$

$$\frac{dT}{dt} = a_{14} + \alpha_{15}L + \frac{\alpha_{16}L + \alpha_{17}L^2}{1 + \alpha_{18}L + \alpha_{19}L^2 + \alpha_{20}RT + \alpha_{21}RLT} - \alpha_{22}T \quad (6)$$

where R , L , and T are concentrations of GnRH, LH (above the basal level), and testosterone, respectively. The first term in eq. 4 accounts for the autoregulatory effect of GnRH and T on GnRH secretion. The second term represents the removal of GnRH proportional to the amount present, and similarly for all the last terms in eqs. 4–6.

The factor $a_{10}R$ in eq. 5 accounts for the stimulating effect of GnRH on the release of LH, while a_9 accounts for the autonomous secretion of LH independent of GnRH. The term $\alpha_{15}L$ in eq. 6 accounts for the stimulating effect of LH on testosterone secretion, while a_{14} is the secretion rate of T independent of LH. The factors in the denominators of the positive terms in the 3 equations account for autoregulation on the rates of secretion of all 3 hormones.

Taking into account the cascade effect of the system described earlier, we can assume that the time responses of the three components in the above system are quite diversified, and scale the dynamics of the cascade by means of two small dimensionless positive parameters ε and δ as follows. Letting

$x = R$, $y = \varepsilon L$, $z = \varepsilon \delta T$, $a_4 = \frac{\alpha_4}{\varepsilon \delta}$, $a_5 = \frac{\alpha_5}{\varepsilon^2 \delta^2}$, $a_{11} = \frac{\alpha_{11}}{\varepsilon \delta}$, $a_{13} = \frac{\alpha_{13}}{\varepsilon}$, $a_{15} = \frac{\alpha_{15}}{\varepsilon}$, $a_{16} = \frac{\alpha_{16}}{\varepsilon}$, $a_{17} = \frac{\alpha_{17}}{\varepsilon^2}$, $a_{18} = \frac{\alpha_{18}}{\varepsilon}$, $a_{19} = \frac{\alpha_{19}}{\varepsilon^2}$, $a_{20} = \frac{\alpha_{20}}{\varepsilon \delta}$, $a_{21} = \frac{\alpha_{21}}{\varepsilon^2 \delta}$, and $a_{22} = \frac{\alpha_{22}}{\varepsilon \delta}$, we are led to the following system.

$$\frac{dx}{dt} = \frac{a_1 + a_2x + a_3x^2}{1 + a_4z + a_5z^2 + a_6x + a_7x^2} - a_8x \equiv f(x, y, z) \quad (7)$$

$$\frac{dy}{dt} = \varepsilon \left[\frac{a_9 + a_{10}x}{1 + a_{11}z + a_{12}x} - a_{13}y \right] \equiv \varepsilon g(x, y, z) \quad (8)$$

$$\frac{dz}{dt} = \varepsilon \delta \left[a_{14} + a_{15}y + \frac{a_{16}y + a_{17}y^2}{1 + a_{18}y + a_{19}y^2 + a_{20}xz + a_{21}xyz} - a_{22}z \right] \equiv \varepsilon \delta h(x, y, z) \quad (9)$$

We are able to show that the relative positions of the 3 equilibrium manifolds $f = 0$, $g = 0$ and $h = 0$ will be as depicted in Fig. 3 if the following conditions hold:

$$a_8 < a_2 \quad (10)$$

$$a_6a_8 - a_3 < 0 \quad (11)$$

$$a_{15}a_{18}^2 + a_{17}a_{18} + 2a_{15}a_{19} > a_{16}a_{19} \quad (12)$$

$$27q^2 + 4p^3 < 0 \quad (13)$$

$$4u^3 + 27v^2 > 0 \quad (14)$$

$$y_1 < y_m \text{ and } y_M < y_2 \quad (15)$$

where

$$p = \frac{s^2}{3} \quad (16)$$

$$q = t + \frac{2s^3}{27} \quad (17)$$

$$s = \frac{a_6a_8 - a_3}{2a_7a_8} \quad (18)$$

$$t = \frac{a_1}{2a_7a_8} \quad (19)$$

$$u = c_2 - \frac{c_1^2}{3} \quad (20)$$

$$v = c_3 - \frac{c_1c_2}{3} + \frac{2c_1^3}{27} \quad (21)$$

$$c_1 = \frac{a_6a_8 - a_3}{a_7a_8} \quad (22)$$

$$c_2 = \frac{a_8 - a_2}{a_7 a_8} \tag{23}$$

$$c_3 = -\frac{a_1}{a_7 a_8} \tag{24}$$

while y_1, y_2 are the y -coordinates of the minimum and maximum points, respectively, on the $f = g = 0$ curve, and y_m, y_M are those of the $f = h = 0$ curve, as seen in Fig. 3. Specifically, inequality (15) is the separation condition which ensures that the slow manifold $h = 0$ separates the two stable branches of the curve $f = g = 0$ for y in a certain interval containing the point where $f = g = h = 0$.

The system, initially at a generic point, say point A of Fig. 3, will make a fast $O(1)$ transition, indicated by three arrows, to the stable portion of the slow manifold $f = 0$ (point B in Fig. 3). As point B is approached, y has slowly become active. An $O(\epsilon)$ transition at intermediate speed, indicated by two arrows, is made along $f = 0$ in the direction of decreasing y , since $g > 0$ here, to point C on the stable part of the curve $f = g = 0$. From point C, a slow $O(\epsilon\delta)$ transition, indicated by a single arrow, is then made along this curve in the direction of increasing z , since $h > 0$ here below the surface $h = 0$.

Once point D is reached, the stability of the manifold is lost. The $O(1)$ time-scale becomes dominant once again. Hence, the orbit follows a path close to the curve $y = \text{constant}$, $z = \text{constant}$, at high speed, bringing the system to point E on the other stable branch of the manifold $f = 0$. This is followed by a motion at intermediate speed on $f = 0$ to point F on the curve $f = g = 0$. Consequently, the system will slowly develop along this line in the direction of decreasing z , since h is now negative.

At point G on this curve, the stability will again be lost and a fast transition will bring the system back to point H on the stable portion of $f = 0$, followed by a motion at intermediate speed to point I on the curve $f = g = 0$, before repeating the same previously described path, thereby forming a closed cycle IDEFGHI. Thus, the existence of a limit cycle in the system for ϵ and δ sufficiently small is assured. The exact solution trajectory of the system will be contained in a tube about this closed curve, the radius of which tends to zero with ϵ and δ .

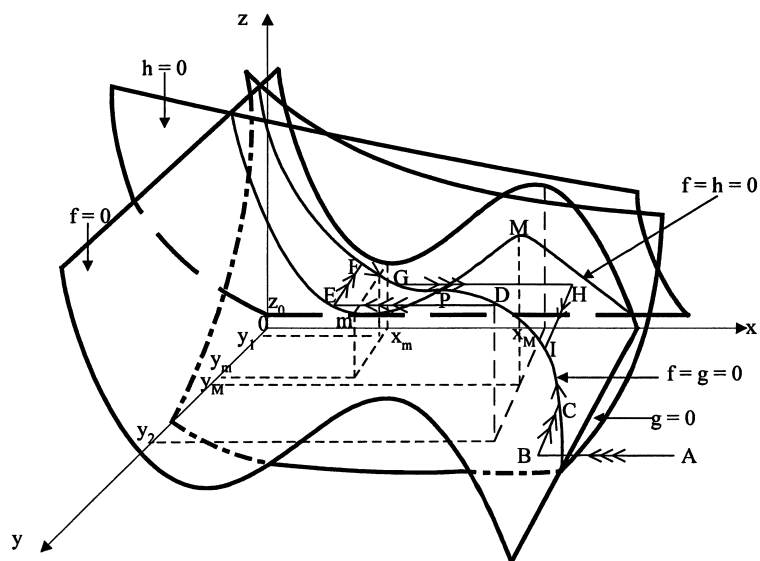


Fig. 3 Shapes and relative positions of the equilibrium manifolds in the case where a limit cycle exists. Here, three arrows indicate fast transitions, two arrows indicate transitions at intermediate speed, and a single arrow indicates slow transitions.

A computer simulation of eqs. 7–9 is presented in Fig. 4 with parametric values chosen to satisfy the inequalities (10–15). The solution trajectory, projected onto the (y, x) -plane, is seen in Fig. 4a to tend to a limit cycle as theoretically predicted. The corresponding periodic time series of LH is shown in Fig. 4b.

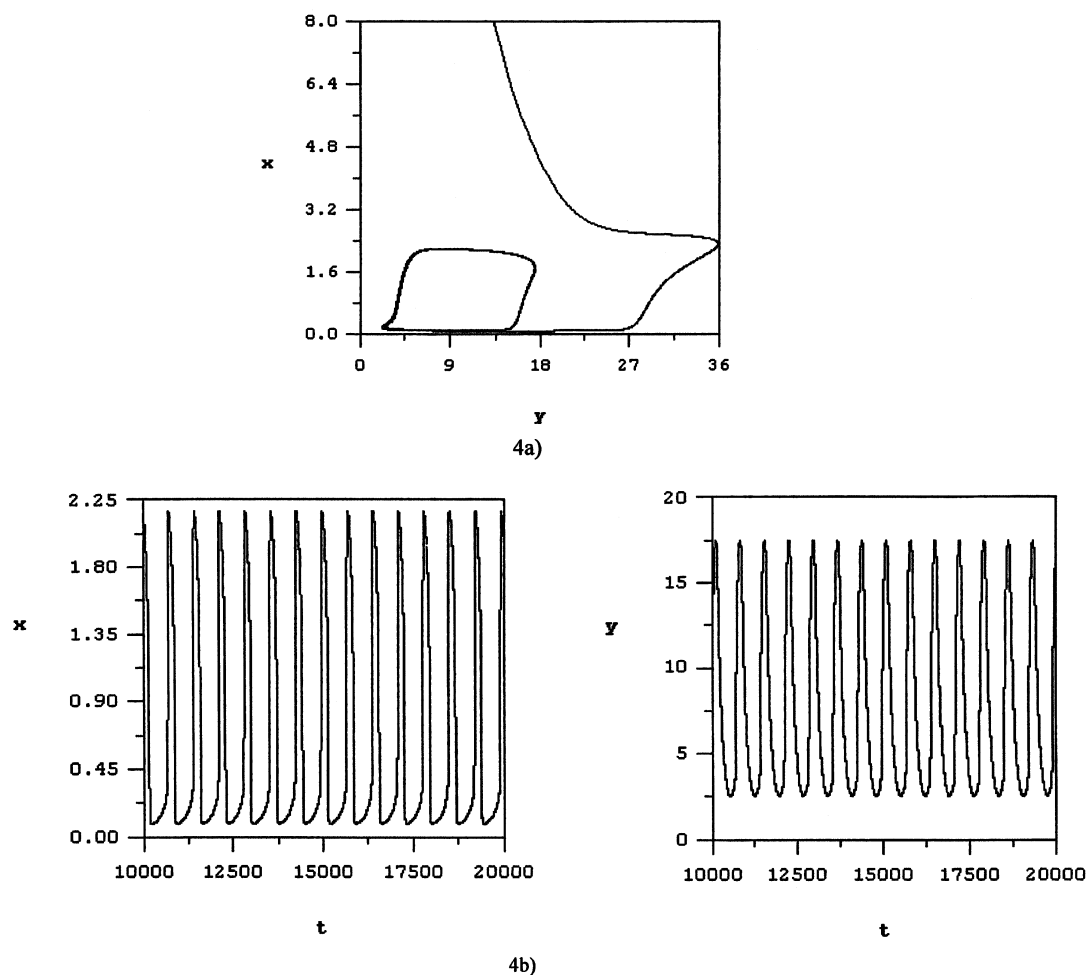


Fig. 4 A computer simulation of the model system of eqs. 7–9 with parametric values chosen to satisfy the conditions identified in the text for which periodic solutions exist. The solution trajectory, projected onto the (y,x) -plane, is seen in (a) to tend toward a stable limit cycle as theoretically predicted. The corresponding time series of GnRH (x) and LH (y) are shown in (b). Here, $\varepsilon = 0.8$, $\delta = 0.05$, $a_1 = 0.2$, $a_2 = 0.1$, $a_3 = 3$, $a_4 = 0.1$, $a_5 = 0.01$, $a_6 = 0.5$, $a_7 = 2$, $a_8 = 0.5$, $a_9 = 0.05$, $a_{10} = 1.5$, $a_{11} = 1.0$, $a_{12} = 0.2$, $a_{13} = 0.01$, $a_{14} = 0.2$, $a_{15} = 0.1$, $a_{16} = 0.1$, $a_{17} = 0.1$, $a_{18} = 0.2$, $a_{19} = 0.2$, $a_{20} = 0.1$, $a_{21} = 0.1$, and $a_{22} = 0.1$.

Extension to higher-dimensional systems

In order to extend the above concept to higher dimensional systems, let us consider a system of $n + 3$ differential equations which may be written in the form

$$\dot{x} = F(x, y, z, w; \alpha) \quad (25)$$

$$\dot{y} = \varepsilon G(x, y, z, w; \alpha) \quad (26)$$

$$\dot{y} = \varepsilon \delta H(x, y, z, w; \alpha) \quad (27)$$

$$\dot{w} = \varepsilon \delta \eta K(x, y, z, w; \alpha) \quad (28)$$

where ε , δ , and η are small positive constants, $\alpha \in \mathfrak{R}^N$ is the N -dimensional vector of system parameters,

while $\begin{bmatrix} x \\ y \\ z \end{bmatrix} \in \mathfrak{R}^3$ and

$$w = \begin{bmatrix} w_1 \\ w_2 \\ \vdots \\ w_n \end{bmatrix} \in \mathfrak{R}^N$$

are the $n + 3$ state variables, and

$$K = \begin{bmatrix} K_1(x, y, z, w; \alpha) \\ K_2(x, y, z, w; \alpha) \\ \vdots \\ K_n(x, y, z, w; \alpha) \end{bmatrix}$$

Hence, x is the fast variable, y the intermediate, z the slow, and w_i , $i = 1, 2, \dots, n$, the very slow components of the system.

Employing the same line of arguments as above, we first assume that w is varying extremely slowly in comparison to the first three components x , y , and z . Then, we may initially assume that w is kept frozen at a constant value $w(0)$ while x , y , and z vary according to the three-dimensional system

$$\dot{x} = F[x, y, z, w(0); \alpha] = f(x, y, z) \quad (29)$$

$$\dot{y} = \varepsilon G[x, y, z, w(0); \alpha] = \varepsilon g(x, y, z) \quad (30)$$

$$\dot{y} = \varepsilon \delta H[x, y, z, w(0); \alpha] = \varepsilon \delta h(x, y, z) \quad (31)$$

Thus, if, for suitable parametric values α , the relative positions of the three equilibrium manifolds of the system (29–31) are the same as those three shown in Fig. 3, then trajectories will develop as described earlier. However, as w varies with time, though very slowly, the shapes and positions of the three manifolds shift slowly as time passes. The coordinates of the points m , M , and O are, in this case, $[x_m(w; \alpha), y_m(w; \alpha), z_m(w; \alpha)]$, $[x_M(w; \alpha), y_M(w; \alpha), z_M(w; \alpha)]$, and $[x_o(w; \alpha), y_o(w; \alpha), z_o(w; \alpha)]$ respectively, since F , G , and H are all functions of w .

Moreover, if we further assume that each of the equations

$$K_i(x, y, z, w; \alpha) = 0, \quad i = 1, 2, \dots, n, \quad (32)$$

can be solved for z as an explicit function of the other components:

$$z = Z_i(x, y, w; \alpha), \quad i = 1, 2, \dots, n, \quad (33)$$

then separation conditions are needed to ensure that the manifold $H = 0$, as well as those described by the equations in (33) are positioned in between the two stable branches of the curve $F = G = 0$, in order that a limit cycle exists. These conditions are stated in the following theorem, under all the assumptions mentioned above.

Theorem: Suppose that the functions $F(x, y, z, w; \alpha)$, $G(x, y, z, w; \alpha)$, $H(x, y, z, w; \alpha)$, and $K(x, y, z, w; \alpha)$, are continuous, and that the functions $x_M(w; \alpha), z_M(w; \alpha)$, $x_m(w; \alpha), z_m(w; \alpha)$, $x_O(w; \alpha), z_O(w; \alpha)$, and Z_i , $i = 1, 2, \dots, n$, are continuous and bounded. If, for some permissible value of α , and each fixed value of w , there exists a unique equilibrium point O, where $F = G = H = 0$, and $K = 0$, such that

$$\sup_w x_m(w; \alpha) < \inf_w x_O(w; \alpha) \quad (34)$$

$$\sup_w x_O(w; \alpha) < \inf_w x_M(w; \alpha) \quad (35)$$

$$\sup_w z_m(w; \alpha) < \min_i \inf_{\Delta_i} Z_i \quad (36)$$

$$\max_i \sup_{\Delta_i} Z_i < \inf_w z_M(w; \alpha) \quad (37)$$

where the supremum and infimum of Z_i are taken over its domain Δ_i which is a subset of \mathfrak{R}^{n+2} , then a limit cycle exists for the system of eqs. 25–28, provided that ε , δ , and η , are sufficiently small.

CONCLUSION

Analysis of a self-regulatory endocrine system that incorporates a cascade mechanism has been elucidated through modeling and arguments based on the singular perturbation principles that have exploited the highly diversified dynamics of the cascade system. The method decomposes the system into fast, intermediate, and slow components. The slow-motion trajectories lie on the equilibrium manifold of the fast component. The existence of limit cycles characterized by fast transitions between stable equilibria gives rise to periodic solutions. Thus, the temporal secretion patterns often observed in clinical data [1,2] appear to be the effect of the inherent cascade mechanism combined with the mixture of negative and positive feedback autoregulation process, giving rise to a natural frequency in the pulsatile mode of secretion. When this is interfered with by signals from the neural components or other external factors, irregular secretion patterns may result which have been frequently observed clinically [1,2].

The above analysis provides an example of how episodic activities in a cascade system may be modeled and explained. The technique has then been extended to higher-dimensional systems in order to be capable of coping with multiple-component cascades.

ACKNOWLEDGMENT

Appreciation is extended to the Thailand Research Fund for the financial support that made this research project possible (contract number RTA/02/2542 and PHD/0029/254).

REFERENCES

1. L. L. Ewing and B. Zirkin. *Recent Prog. Hormone Res.* **39**, 599–632 (1983).
2. R. V. Gallo. *Biol. Reprod.* **24**, 771–777 (1981).
3. S. Muratori and S. Rinaldi. *Siam. J. Appl. Math.* **52**, 1688–1706 (1992).
4. Y. Lenbury, K. Kamnungkit, B. Novaprateep. *IMA J. Math. Applied Med. Biol.* **13**, 1–21(1996).
5. Y. Lenbury, R. Ouncharoen, N. Tumrasvin. *IMA J. Math. Applied Med. Biol.* **17**, 243–261(2000).
6. B.-Z. Liu and G.-M. Deng. *J. Theor. Biol.* **150**, 51–58 (1991).